esa

ECOSPHERE

Tropical forest temperature thresholds for gross primary productivity

STEPHANIE PAU [1,†] MATTEO DETTO [2,3] YOUNGIL KIM [4] AND CHRISTOPHER J. STILL [4]

[1]*Department of Geography, Florida State University, 113 Collegiate Loop, Tallahassee, Florida 32306 USA*
[2]*Smithsonian Tropical Research Institute, Apartado 0843–03092, Balboa, Ancón, Panama*
[3]*Department of Ecology and Evolutionary Biology, Princeton University, Princeton, New Jersey 08544 USA*
[4]*Department of Forest Ecosystems and Society, Oregon State University, Corvallis, Oregon 97331 USA*

Citation: Pau, S., M. Detto, Y. Kim, and C. J. Still. 2018. Tropical forest temperature thresholds for gross primary productivity. Ecosphere 9(7):e02311. 10.1002/ecs2.2311

Abstract. Tropical forests are hyper-diverse and perform critical functions that regulate global climate, yet they are also threatened by rising temperatures. Canopy temperatures depart considerably from air temperatures, sometimes by as much as air temperatures are projected to increase by the end of this century; however, canopy temperatures are rarely measured or considered in climate change analyses. Our results from near-continuous thermal imaging of a well-studied tropical forest show that canopy temperatures reached a maximum of ~34°C, and exceeded maximum air temperatures by as much as 7°C. Comparing different canopy surfaces reveals that bark was the warmest, followed by a deciduous canopy, flowers, and coolest was an evergreen canopy. Differences among canopy surfaces were largest during afternoon hours, when the evergreen canopy cooled more rapidly than other canopy surfaces, presumably due to transpiration. Gross primary productivity (GPP), estimated from eddy covariance measurements, was more strongly associated with canopy temperatures than air temperatures or vapor pressure deficit. The rate of GPP increase with canopy temperatures slowed above ~28–29°C, but GPP continued to increase until ~31–32°C. Although future warming is projected to be greater in high-latitude regions, we show that tropical forest productivity is highly sensitive to small changes in temperature. Important biophysical and physiological characteristics captured by canopy temperatures allow more accurate predictions of GPP compared to commonly used air temperatures. Results suggest that as air temperatures continue to warm with climate change, canopy temperatures will increase at a ~40% higher rate, with uncertain but potentially large impacts on tropical forest productivity.

Key words: canopy temperature; climate change; ecosystem function; productivity; thermal imaging; tropical forest.

Received 14 May 2018; accepted 18 May 2018. Corresponding Editor: Debra P. C. Peters.

† **E-mail:** spau@fsu.edu

INTRODUCTION

The Earth's temperature is rapidly warming with rising anthropogenic CO_2 concentrations in the atmosphere (IPCC 2014). Global mean air temperatures for the end of the twentieth century are projected to increase between 0.3 and 1.7°C to as high as 2.6–4.8°C relative to 1986–2005 temperatures (IPCC 2014). Important differences in projected future air temperature patterns exist between high-latitude (boreal and sub-arctic), temperate, and tropical regions. Critically, tropical regions may experience air temperatures well outside of their historical range much sooner (Battisti and Naylor 2009, Diffenbaugh and Scherer 2011, Mora et al. 2013).

Tropical species may be especially sensitive to rising temperature because they have evolved within a narrow temperature range and furthermore exist closer to their upper temperature

maxima (Janzen 1988, Ghalambor et al. 2006, Tewksbury et al. 2008, Wright et al. 2009). Recent work has highlighted temperature as having large effects on tropical forest growth and mortality, ecosystem function, and species distributions. In Costa Rica, tree mortality was associated with higher nighttime air temperatures (Clark et al. 2010). In the Amazon, leaf-level photosynthesis and whole-canopy CO_2 uptake decreased when leaf temperatures exceeded 35°C (Doughty and Goulden 2008). Multiple components of net primary productivity (NPP) have been shown to be sensitive to temperature, from the negative effects on woody tree growth in Costa Rica (Clark et al. 2010, 2013) and the Amazon (Toomey et al. 2011), to the positive effects on flower production in Panama associated with El Niño events (Pau et al. 2013, 2018). The decrease in woody growth in Costa Rica was associated with nighttime air temperatures above ~21°C, consistent with an increase in nighttime plant respiration (Clark et al. 2003, 2010). However, leaf respiration can acclimate to higher temperatures when experimentally warmed (Slot et al. 2014), and higher nighttime temperatures can stimulate seedling growth despite an increase in leaf dark respiration (Cheesman and Winter 2013).

Organismal temperatures are rarely considered or quantified in climate change projections, even though the actual temperatures experienced by organisms often depart from air temperatures. Indeed, organismal temperatures determine physiological, biochemical, and metabolic responses and thus are critical in shaping patterns of biodiversity, biogeography, and climate sensitivity (Tewksbury et al. 2008, Fisher et al. 2011, Still et al. 2014). In forest ecosystems, canopy temperatures, while coupled to air temperatures, are known to diverge from air temperatures because of radiative energy exchanges and strong ecophysiological controls such as leaf characteristics (stomatal controls on transpiration, leaf size, shape, pubescence, and angle) and canopy architecture (e.g., height of the canopy, density, roughness), which together affect heat and water exchanges (Jones 1992, Leuzinger and Körner 2007). Critically, many important canopy processes, like photosynthesis, respiration, and transpiration, vary nonlinearly with canopy temperature, and thus assuming leaves are at air temperature can lead to large errors.

Empirical work on leaf temperatures using measurements from thermocouples tends to be species-specific and/or short-term (Doughty and Goulden 2008, Rey-Sánchez et al. 2016). An alternative to leaf- and time-specific temperature measurements is the use of land surface temperature (LST) products from satellites. Land surface temperature is based on the thermal infrared radiation measured by satellite radiometers, which are capable of providing data across different ecosystems and seasons (Vancutsem et al. 2010). Comparisons have shown that denser canopies are typically cooler than sparser vegetation because of larger latent heat fluxes, and that evaporative cooling can occur even during dry periods if roots are able to access groundwater to maintain transpiration in the canopy (Vancutsem et al. 2010, Mildrexler et al. 2011). The contribution of much hotter soils and more bare ground in mixed pixels is also a potential contributor to higher temperatures observed in sparser canopies from satellite data (Mildrexler et al. 2011). By contrast, site-level thermal cameras that capture just the canopy have shown that denser canopies from temperate broad-leaved trees are in fact warmer than sparser canopies, by up to 5°C (Leuzinger and Körner 2007, Aubrecht et al. 2016), highlighting the complexity of canopy thermal regimes.

Tropical forests may experience less climatic variability than other biomes; however, their high species diversity and complex forest canopy structure can result in highly variable microclimates. The vulnerability of tropical forests to climate change is critically important because these habitats are among the most diverse in the world, and store and cycle large amounts of carbon (Pan et al. 2011). For these reasons, accurate and spatially resolved measurements are needed to understand tropical forest responses to changes in temperature. Advances in in situ sensing have recently gained attention by providing species-specific information in their natural habitats and critical links to larger scale monitoring from airborne and satellite measurements (Turner 2014). Here, we present results from in situ, near-continuous thermal camera monitoring and eddy flux measurements of gross primary productivity (GPP)—which represents the

gross rate of carbon fixed by the forest during photosynthesis—at a tropical forest site in Barro Colorado Island (BCI), Panama. We address two primary questions with the goal of better understanding canopy temperatures: (1) How do canopy temperatures, including differences within the canopy and throughout the day, depart from more commonly examined air temperatures? and (2) What is the relationship between canopy temperatures and GPP?

Methods

Study site and instrumentation

Barro Colorado Island, Panama, is located at 9°10′ N, 79°51′ W. Barro Colorado Island is a well-studied tropical moist forest with more than 2200 plant species, about 300 tree and shrub species including ~12% deciduous broadleaf tree species (Croat 1978). The site experiences annual rainfall averages of 2642 (± 566) mm with a pronounced dry season from January to April. In our record, we captured the dry season from February to April and the wet season from May to September. Species in the camera field of view (FOV) include, among others: *Gustavia superba* (leaves simple, 1 m long, evergreen), *Hura crepitans* (leaves simple, 11–25 cm long, deciduous), *Inga pezizifera* (compound leaves, leaflets 8–2 cm long, evergreen), *Platypodium elegans* (compound leaves, leaflets 2.5–7.5 cm long, deciduous), *Spondia mombin* (leaves pinnate, up to 60 cm long, deciduous), *Spondia radlkoferi* (leaves pinnate, up to 54 cm long, deciduous), *Tabebuia guayacan* (leaves palmate, 9–30 cm long, deciduous), *Tabebuia rosea* (leaves palmate, 5–25 cm long, deciduous), *Platymiscium pinnatum* (compound leaves, leaflets 5–11 cm long, deciduous), *Sterculia apetala* (leaves palmate, 35 cm long, deciduous), and *Virola surinamensis* (leaves simple, 9–16 cm long, evergreen).

A thermal camera (FLIR A325sc, FLIR System, Wilsonville, Oregon, USA) was installed on a telecommunications tower 40 m above ground (10 m above mean canopy height) facing southwest to capture near-continuous thermal infrared (TIR) images (Appendix S1: Fig. S1). The camera was housed in a FLIR F-Series waterproof enclosure (with a Germanium window that transmits >99% of longwave radiation) to protect it from ambient moisture and precipitation. The camera uses an uncooled microbolometer detector to measure photons in the 7.5–13 μm spectral range with a pixel resolution of 360 × 240. A FLIR IR 18 mm lens (focal length: 18.0 mm; FOV: 25° × 18.8°) was used for image collection. Within the FOV, a single pixel spot size is 0.14 cm from 1 m, 1.4 cm from 10 m, 6.9 cm from 50 m, and 20.8 cm from 150 m in a single pixel. FLIR ResearchIR Max software was used following methods described in Kim et al. (2016).

Aubrecht et al. (2016) showed that camera error is <1°C at air temperatures as high as 30°C, irrespective of relative humidity. At air temperatures above 30°C and relative humidity as high as 80%, tests showed that camera error remained below 2°C. Camera errors are primarily related to the fixed parameters (e.g., emissivity, reflected apparent temperature, and atmospheric temperatures) and calibration processes in the camera and software (Minkina and Dudzik 2006). Of these fixed parameters, emissivity appears to contribute the most error (Aubrecht et al. 2016). However, for emissivity values between 0.94 and 0.96, which is reasonable for most vegetation, the error is ~1°C (Aubrecht et al. 2016). Furthermore, if several objects are of similar distances from the camera, the information on relative temperature differences should be accurate compared to their absolute temperatures (Faye et al. 2016, see Kim et al. 2016 for further detail). Distances of canopy surface types selected for analyses (deciduous canopy, evergreen canopy, flowers, and bark), measured with a laser range finder, were 57 m, 51 m, 143 m, and 57 m, respectively. Aubrecht et al. (2016) found a small effect of distance on an object's retrieved temperatures, although increased distance affected the minimum size of the smallest resolved object and also the homogeneity of surfaces in a region of interest. Thus, the comparison between the deciduous canopy, evergreen canopy, and bark is the most robust, whereas comparisons with flowers have the most uncertainty, as they may include other canopy elements in addition to flowers.

Thermal infrared images were collected every 5 min from 17 February to 30 September 2015, resulting in 288 images per day, which captured the beginning of the 2015 El Niño event. Due to power failures, continuous measurements were interrupted between 3 August and 6 August

2015. In total, 5198 images were captured over 257 d. To our knowledge, this is the longest thermal record from any tropical forest.

Meteorological variables and turbulent fluxes were measured from a 45-m flux tower located in the FOV of the camera (Fig. 1 and Appendix S1: Table S1). Air temperature and RH were measured by a HC2S3 probe (Campbell Scientific, Logan, Utah, USA) enclosed in a radiation shield. Vapor pressure deficit (VPD; Pa) was calculated using RH, and either T_{air} or T_{can}, following Jacobson (2002). The four components of radiation were measured with a CNR1 and a CMP11 pyranometer (Kipp & Zonen, The Netherlands). Net radiation (R_{net}, W/m^2) was obtained as the difference between the sum of incoming shortwave and longwave radiations and the sum of upwelling longwave and reflected shortwave radiations. Photosynthetically active radiation (PAR) was measured using a sunshine sensor (BF5, Delta-T Devices, UK). These variables were sampled every 5 s and stored as 5-min averages. Sensible heat (H, W/m^2), latent heat (LE, W/m^2), and CO_2 fluxes (net ecosystem exchange [NEE], $\mu mol \cdot m^{-2} \cdot s^{-1}$) were obtained from an eddy covariance system equipped with CSAT3 sonic anemometer (Campbell Scientific) and a LI-7500 open-path gas analyzer (Li-Cor, Lincoln, Nebraska, USA) located at 41 m from the ground. The sampling rate of the eddy covariance system was 10 Hz, and fluxes were computed on a 30-min averaging window using a standard routine described in Detto et al. (2010). Prior to computing the fluxes, a de-spiking algorithm was applied to detect and remove spikes in raw data (values greater than six standard deviations in a one-minute window), bad readings exceeding a reasonable physical range, and low diagnostic instrument values. A QA/QC procedure was applied to the 30-min turbulent fluxes to remove measurements during and immediately after rain events, unreasonable physical values, or not satisfying other turbulent criteria (Appendix S1: Table S2). Gross primary productivity ($\mu mol \cdot m^{-1} \cdot s^{-1}$) was derived by subtracting NEE from ecosystem respiration (RECO), GPP = RECO-NEE. RECO was estimated as the intercept of the NEE-light response curve (Lasslop et al. 2010) computed on a 3-d moving window using only daytime fluxes with friction velocities larger than 0.4 m/s.

In order to compute daily time integrated budgets, gaps were filled using Artificial Neural Network (Papale and Valentini 2003) with hydro-meteorological inputs as predictors (soil moisture, solar radiation, temperature, VPD, and air pressure). To train the network, the dataset was randomly divided into a training set (70%), a validation set (15%), and a test set (15%). A two-layer feed-forward network with 10 sigmoid hidden neurons and linear output neurons was trained using the Levenberg-Marquardt algorithm until the mean square

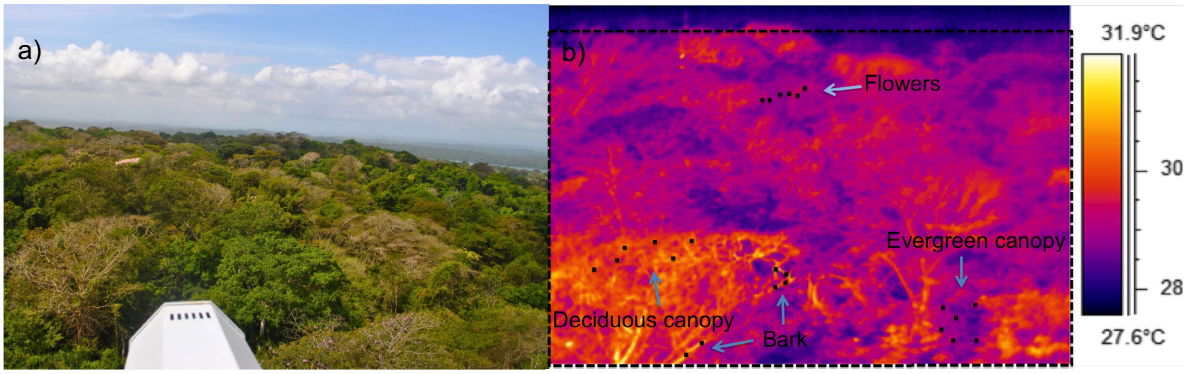

Fig. 1. Photograph of the forest canopy on Barro Colorado Island during the dry season and the thermal camera in the foreground, mounted on a 40 m tower facing northwest, and the eddy flux tower in the background (a). Thermal image of the forest canopy (b). Dotted black line is the cropped image used for T_{can} values, while black squares are regions of interest (each 2 × 2 pixels) used to extract values for different canopy surfaces (a deciduous canopy, evergreen canopy, flowers, and bark). Both images taken on 17 February 2015.

error (MSE) of the validation set stop improving (Hagan and Menhaj 1994). Performance, in term of MSE, was evaluated using the test set at the end of the training. This procedure was repeated 100 times to produce 100 estimates of GPP. Training multiple times generates different results due to different initial conditions and random sampling of the three sets. Ensemble was obtained as weighted average from the 100 ANN predictions using the MSE of the test set as weights according to:

$$f_i = \frac{\sum_k f_{ik}^{\mathrm{ANN}}/\mathrm{MSE}_{ik}}{\sum_k 1/\mathrm{MSE}_{ik}}$$

The ANN was implemented using the Neural Network Toolbox in Matlab 2014a (The MathWorks, Inc., Natick, Massachusetts, USA).

Canopy surface types and statistical analysis

To compare canopy temperatures (T_{can} from the entire FOV) to air temperatures (T_{air}), 5-min TIR and climate data were averaged to half-hourly, hourly, or daily means. To examine spatial and species variability in T_{can}, different canopy surface types were selected corresponding to a deciduous tree canopy (*P. elegans*), an evergreen tree canopy (unidentified), flowers (from a liana in the crown of *H. crepitans*), and bark (*P. elegans*). Canopy surface values used in analyses were averages of six regions of interest (ROIs) for each surface type (Fig. 1). Each ROI was 2 × 2 pixels (distances provided above; effective pixel sizes ranged between ~7 [leaves and bark] and 20 cm [flowers]). To examine temporal variability in T_{can}, data were averaged to morning (04:00–11:59), afternoon (12:00–19:59), and nighttime (20:00–23:59 and 0:00–03:59) values, following Kim et al. (2016).

Pearson's correlations were used to examine the strength and direction of relationships between T_{can} and T_{air}, as well correlations with meteorological, radiation, and flux variables (T_{air}, H, LE, RH, SW_{dn}, R_{net}, VPD). To examine non-linear relationships between either metric of temperature (T_{can} and T_{air}) and GPP, we used piecewise regressions of half-hourly mean data. We compared linear models and piecewise models (with breakpoints that resulted in the lowest residual error) using Akaike's Information Criterion (AIC), which penalizes for the number of model parameters. Models with ΔAIC < 2 are considered equivalent best-fit models (Burnham and Anderson 2002).

Results

Comparisons with air and leaf temperatures

Canopy temperatures (T_{can}) were on average 1.6°C warmer than air temperatures (T_{air}) on a daily basis and as much as 1.9°C warmer than T_{air} in hourly averaged data (Fig. 2). For every 1.0°C increase in T_{air}, T_{can} increased 1.4°C on average using all day data ($r^2 = 0.90$, $P < 0.001$, $n = 4192$). When examining only morning data, T_{can} increased 1.5°C for every 1.0°C increase in T_{air}, while afternoon only data had a smaller increase (1.4°C for every 1.0°C increase in T_{air}). Nighttime data had the smallest increase (1.1°C for every 1.0°C increase in T_{air}). Morning T_{can} rose quickly with increasing R_{net} from nighttime lows when T_{can} and T_{air} were more similar, whereas afternoon T_{can} was closer to T_{air} and

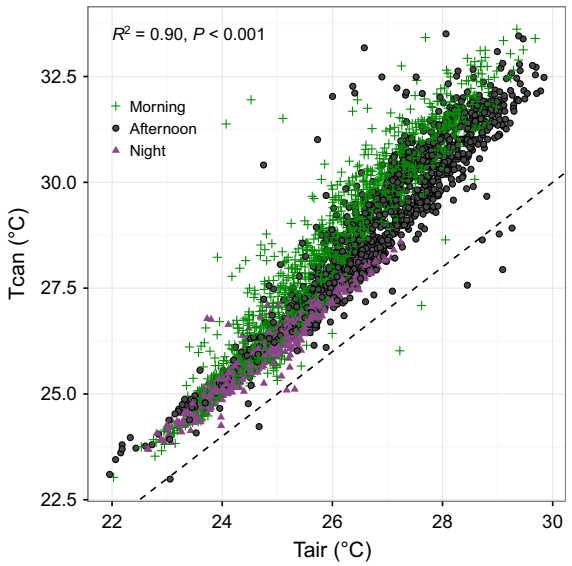

Fig. 2. Relationship between air temperatures (T_{air}) and canopy temperatures (T_{can}). T_{can} is on average 1.9°C warmer than T_{air} in hourly data, but departures are greater at higher temperatures during morning (04:00–11:59) and afternoon (12:00–19:59) hours, and smaller at night (0:00–03:59; 20:00–23:59). All data: β = 1.4, $r^2 = 0.90$, $P < 0.001$; morning: β = 1.5, $r^2 = 0.90$, $P < 0.001$; afternoon: β = 1.3, $r^2 = 0.88$, $P < 0.001$.

declined more slowly to nighttime temperatures (Fig. 3). Peak T_{can} occurred in late morning, at 11:00. The warmer morning T_{can} matched a lower Bowen ratio (morning median = 0.65), indicating greater latent heat flux, whereas greater sensible heat flux drove higher Bowen ratios (afternoon median = 0.89) likely as stomatal conductance and latent heat flux declined in the afternoon (Fig. 4). Although latent heat fluxes were higher in the morning, the largest T_{can} departures from T_{air} occurred when sensible heat fluxes were higher (Fig. 4).

Average T_{can} mask two modes in the data largely driven by differences in afternoon and nighttime temperatures (Appendix S1: Fig. S1). Mean T_{can} averaged 27.7°C across the entire record, but T_{can} was within 0.5°C of the mean only 19% of the time and within 0.1°C of the mean only 3% of the time. The diurnal temperature range of T_{can} was 5.5°C compared to 3.6°C for T_{air}. The range of T_{can} over the entire record was 23.0–33.6°C (10.6°C range) compared to 22.0–29.8°C for T_{air} (7.8°C range). The maximum difference between T_{air} and T_{can} was 7.4°C, using either 30-min or hourly averages (Appendix S1: Fig. S2).

Spatial and temporal differences in canopy temperatures

There were significant spatial (deciduous, evergreen, flower, and bark) differences in canopy temperatures ($F_{3,\ 16764} = 12.78$; $P < 0.001$; time of day: $F_{2,\ 16765} = 2669.00$, $P < 0.001$). All surfaces were significantly different from each other (post-hoc Tukey's: adj $P < 0.001$) except for bark-flowers and deciduous canopy-flowers (Fig. 3; Appendix S1: Fig. S1). However, the magnitude of differences for mean temperatures across all time periods was small (mean temperatures: deciduous, 28.5°C; evergreen, 28.3°C; bark,

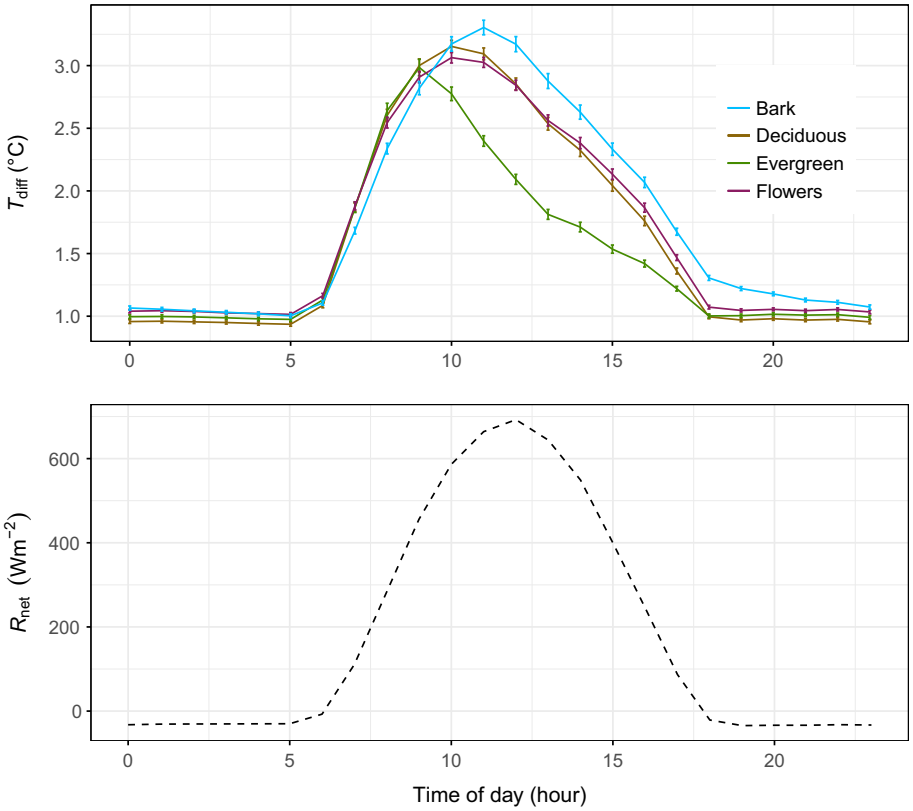

Fig. 3. T_{diff} (T_{can}–T_{air}) for different canopy surfaces averaged from data collected 17 February to 30 September 2015 (January–April is the dry season; May–December is the wet season). The deciduous canopy values combine temperatures from leafless and leafy months to represent average conditions of these species within the canopy.

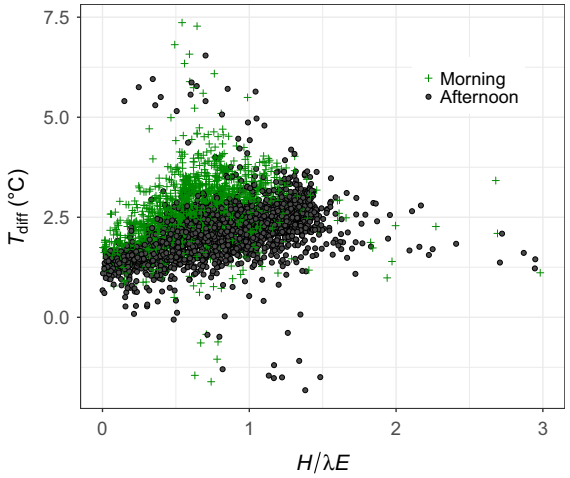

Fig. 4. The relationship between T_{diff} (T_{can}–T_{air}) and the Bowen ratio (H/λE). Morning Bowen ratios were lower (median = 0.65), indicating greater latent heat flux, whereas afternoon values were higher (median = 0.89), indicating greater sensible heat flux.

28.7°C; flowers, 28.6°C). There were also significant temporal (time of day) differences in canopy temperatures ($F_{2,\ 16765} = 2669.00$, $P < 0.001$). All time-of-day groups were also significantly different from each other (post-hoc Tukey's: adj $P < 0.001$). The largest mean difference was between afternoon and nighttime temperatures (mean temperatures: morning, 28.2°C; afternoon, 28.9°C; and night, 26.4°C).

A significant interaction between canopy surfaces and time of day resulted in larger temperature differences; that is, the difference among canopy surfaces depended on the time of day (surface types × time of day: $F_{6,\ 16756} = 8.48$, $P < 0.001$; Appendix S1: Fig. S3). The largest significant differences in canopy surfaces during the same time of day occurred during the afternoon between bark–evergreen canopy (0.7°C on average, maximum of 1.7°C), followed by flowers–evergreen canopy (0.4°C on average, maximum difference of 0.2°C), then deciduous–evergreen canopy (0.4°C on average, maximum difference of 0.5°C), bark–deciduous canopy (0.3°C on average, maximum difference of 1.2°C), and bark–flowers (0.2°C on average, maximum difference of 1.5°C); all post-hoc Tukey's: adj $P < 0.001$).

Correlations showed that all canopy surfaces (deciduous, evergreen, flowers, and bark) were strongly correlated with T_{air}, and relationships were strongest at night (Appendix S1: Table S3). Different canopy surfaces were also similarly correlated with meteorological variables. Bark temperatures were the most elevated above T_{air}, mainly driven by maximum temperature differences (Fig. 3, Appendix S1: Figs. S3, S4).

On average, during morning hours, T_{diff} ($T_{can} - T_{air}$) for all canopy surfaces rose quickly with net radiation (R_{net}), peaking between 09:00 and 11:00, and cooled more slowly in the afternoon (Fig. 3; Appendix S1: Fig. S4). The evergreen canopy peaked earliest in the day, whereas deciduous canopy and bark peaked one to two hours later. Bark tracked R_{net} more closely than other canopy surfaces. The diurnal pattern of T_{can} (i.e., the entire canopy) similarly peaks with R_{net} and appears driven by the diurnal patterns of the deciduous canopy, flowers, and bark more strongly than by the diurnal patterns of the evergreen canopy.

Relationship between canopy temperatures and gross primary productivity

Model comparisons showed that T_{can} consistently resulted in better model-fit of GPP than T_{air} when using linear or piecewise regressions (Table 1, Fig. 5a and 5b). Piecewise regressions to identify non-linear relationships between T_{can} and GPP resulted in better model-fit compared to linear regressions, and also showed that T_{can} was a better predictor of GPP than T_{air}. The best-fit model identified a breakpoint at 28–29°C, when GPP rose fastest with T_{can}. Above 28–29°C, the increase in GPP with T_{can} begins to slow (Table 1; Fig. 5b). Examining relationships by morning or afternoon hours revealed similar breakpoints around 28–29°C during morning hours, above which the rate of GPP increase with T_{can} slowed (Table 2). During the afternoon, GPP declined at T_{can} above 31.6°C; that is, the slope was negative (Table 2, Fig. 5b). However, the decline was not significant in models that excluded gap-filled data (Appendix S1: Table S4). Peak GPP occurred when T_{can} was ~2.5°C above T_{air}, before and after which maximum GPP dropped sharply (Fig. 5c).

T_{can} also resulted in a better model of GPP than VPD in both linear and piecewise regressions (using either VPD calculated with T_{air} [VPD_{tair}] or VPD calculated with T_{can} [VPD_{tcan}]),

Table 1. Model comparisons of T_{can}, T_{air}, and vapor pressure deficit (VPD) to predict gross primary productivity (GPP).

Models of GPP	ΔAIC	k	R^2	β1 (below)	β2 (above)
Tcan (piecewise: 28.6°C)	–	5	0.52	2.36**	2.91***
Tcan (piecewise: 29.2°C)	10.50	5	0.52	2.91*	2.46***
Tcan (piecewise: 32°C)	16.92	5	0.52	3.62***	−0.32 (N.S.)
Tcan (simple linear)	94.02	3	0.51	3.41***	–
Tair (piecewise: 26°C)	639.48	5	0.44	1.74***	4.41***
Tair (piecewise: 28.4°C)	630.70	5	0.44	3.97***	−0.17 (N.S.)
Tair (simple linear)	704.82	3	0.43	4.19***	–
VPDtcan (piecewise: 927 Pa)	1585.26	5	0.30	0.02***	−0.01***
VPDtair (piecewise: 783 Pa)	1609.10	5	0.30	0.02**	0.01***
VPDtcan (simple linear)	2024.92	3	0.22	0.01***	–
VPDtair (simple linear)	2112.11	3	0.20	0.01***	–

Notes: Temperature breakpoints in piecewise models to estimate non-linear relationships were chosen based those that resulted in the lowest residual error. En dash indicates no value.

AIC, Akaike's Information Criterion; k, number of model parameters; R^2, coefficient of determination; β1, slope below breakpoint; β2, slope above breakpoint.

***$P < 0.001$, **$P < 0.01$, *$P < 0.05$, N.S. $P > 0.05$.

which should have a direct effect on GPP via its influence on leaf stomatal conductance (Table 1; Appendix S1: Fig. S5). High rates of GPP were correlated with high LE ($r = 0.77$), high R_{net} ($r = 0.68$), high PAR ($r = 0.67$), high SW_{dn} ($r = 0.67$), high H ($r = 0.62$), and low RH ($r = -0.40$; all correlations had $P < 0.0001$; Appendix S1: Table S5, Fig. S6). Gross primary productivity was more strongly correlated with T_{can} ($r = 0.71$, $P < 0.001$) than with T_{air} ($r = 0.66$, $P < 0.001$) or other meteorological variables, and only the flux variable LE had a higher correlation.

Discussion

Here, we show important differences between T_{can} and more commonly examined T_{air}. We furthermore demonstrate the importance of these differences for more accurately predicting GPP at this tropical forest site in Panama. On average, T_{can} was almost 2°C warmer than T_{air}, but on individual days the offset frequently exceeded 5°C and was as high as 7°C for short time periods. Interestingly, T_{can} remains warmer than T_{air} at night. This is not consistent with nighttime radiative cooling, which drives T_{can} below T_{air}.

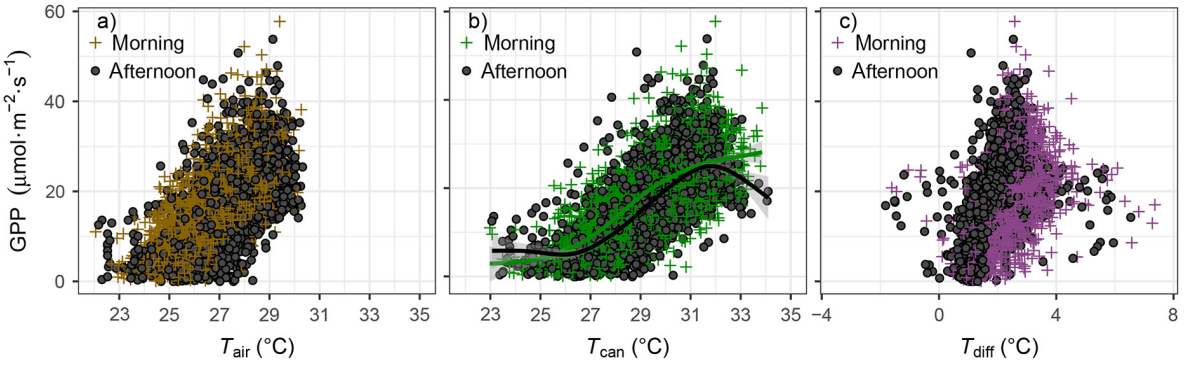

Fig. 5. Relationships between T_{air}, T_{can}, T_{diff} (T_{can}–T_{air}), and gross primary productivity (GPP). T_{air} (a) was a worse-fit model and explained less variability in GPP compared to T_{can} (b; Tables 1 and 2). At T_{can} above 28–29°C, the increase in GPP slowed with increases in T_{can}. The afternoon decline in T_{can} above 31°C (black line) was not significant when excluding gap-filled data. GPP peaked when T_{can} was ~2.5°C above T_{air} (c), and declined below and above 2.5°C.

Table 2. Model comparisons of T_{can} and T_{air} to predict gross primary productivity (GPP) during morning (04:00–11:59) or afternoon (12:00–19:59) hours.

Parameters	ΔAIC	k	R^2	β1 (below)	β2 (above)
Morning					
Tcan (piecewise: 28.6)	–	5	0.60	3.17***	2.43***
Tcan (piecewise: 31.4)	1.38	5	0.60	3.80***	1.00 (N.S.)
Tcan (piecewise: 29.2)	7.70	5	0.60	3.62***	2.11***
Tcan (simple linear)	59.77	3	0.59	3.46***	–
Afternoon					
Tcan (piecewise: 28.8)	–	5	0.48	1.87***	3.04***
Tcan (piecewise: 27.3)	2.07	5	0.48	0.08***	3.76***
Tcan (piecewise: 29.1)	20.23	5	0.48	2.36	2.81***
Tcan (piecewise: 31.6)	21.46	5	0.48	3.63***	−4.17***
Tcan (piecewise: 30.1)	29.18	5	0.48	3.16***	1.39***
Tcan (simple linear)	82.73	3	0.46	3.44***	–

Notes: Temperature breakpoints in piecewise models to estimate non-linear relationships were chosen based those that resulted in the lowest residual error. En dash indicates no value.

AIC, Akaike's Information Criterion; k, number of model parameters; R^2, coefficient of determination; β1, slope below; β2, slope above breakpoint.

***$P < 0.001$, **$P < 0.01$, *$P < 0.05$, N.S. $P > 0.05$.

Nighttime cooling of the canopy is also confirmed by negative sensible heat fluxes at night and in the early morning indicating heat transfer from warmer air into cooler vegetation. This discrepancy might be explained by the complex structure of the tropical forest, heterogeneity of thermal properties of canopy elements, and vertical stratification of the canopy and air temperatures. T_{can} derived from thermal images with shallow angles captures more canopy elements, such as bark and regions of the understory (Figs. 1 and 3), rather than only the upper surface canopy, which is expected to experience radiative heat loss at night. Future investigation into the mechanisms that drive warmer T_{can} at night would provide novel insight into the energy budget of tropical forests.

Differences among canopy surfaces were larger during afternoon hours when the evergreen canopy cooled more rapidly than other canopy surfaces, likely because of latent heat loss. Additionally, the more open deciduous canopy was warmer than the dense evergreen canopy because of the hotter bark exposed during the dry season. In contrast, thermal imaging studies from temperate forests showed that denser canopies from broad-leaved trees were warmer than sparser canopies, possibly owing to the higher transpiration of sparse open canopies (Leuzinger and Körner 2007).

Although we show that tropical forest canopies stay within a much more limited range of temperatures—both temporally and spatially—compared to temperate forests (Leuzinger and Körner 2007, Scherrer and Körner 2011, Aubrecht et al. 2016, Kim et al. 2016), tropical species are thought to live closer to their upper temperature limit and may be more sensitive to temperature variability (Janzen 1988, Ghalambor et al. 2006, Tewksbury et al. 2008, Wright et al. 2009). Differences within the canopy of up to 1.7°C should influence the diversity and distribution of canopy dwelling-species, such as mammals (Briscoe et al. 2014) and ants that experience the very hot temperatures of bark (Kaspari et al. 2015), or epiphytes that partition microhabitats within tropical forest canopies (Woods et al. 2015).

Morning and afternoon hours showed bimodal distributions or, for morning hours, positive skewness (Appendix S1: Fig. S1). Measures of T_{leaf} from Panamanian tree species using thermocouple wires also noted the bimodal distribution of daytime temperatures (Rey-Sánchez et al. 2016, Slot and Winter 2017*b*). Thus, mean values do not accurately capture canopy temperatures, with maximum temperatures in the afternoon driving temperatures away from the mean most frequently.

Although the theoretical leaf energy balance is well understood, complex heat transfer within spatially heterogeneous and temporally dynamic canopies has limited ecological understanding of canopy temperatures (Jones 1992, Leuzinger and Körner 2007, Aubrecht et al. 2016). In addition to lower wind speeds experienced within the canopy, not all leaves within a canopy are exposed to high radiative warming. Although individual leaves in tropical forests can reach temperatures above 40°C, the entire canopy can stay below this value due to the aggregated effect of hot, brightly lit leaves and cooler, less illuminated leaves (Doughty and Goulden 2008).

Our results suggest that as anthropogenic climate change continues to warm our atmosphere, daytime canopy temperatures, which integrate heat and water stress, will experience a 30–50% greater increase than air temperatures. If climate change manifests as drier conditions in Panama, this would limit evaporative cooling that occurs in morning, and canopy temperatures may reach a

high temperature threshold earlier in the day. Our empirical study identified a temperature threshold between 28 and 29°C (averaged across the entire canopy), at which point the rate of GPP increase with temperature declined, though GPP itself was still increasing. The decline in GPP during the afternoon at ~ 31°C was not significant when excluding gap-filled GPP data; however, this may result from a Type II error (there were only 37 data points above 31°C without gap-filled data, but these high temperatures may become more common in the future). Very similar leaf temperature thresholds for photosynthesis of 29.8°C in a wet forest in Panama and 30.8°C in a seasonally dry forest in Panama (similar to BCI) have been documented (Slot and Winter 2017*a*), as well as 30–30.5°C in a Brazilian tropical forest (Doughty and Goulden 2008, Doughty 2011).

While our observational study has revealed existing relationships between T_{can} and GPP, extrapolating correlative relationships for future predictions can be highly uncertain. For example, incoming solar radiation, a strong influence on T_{can}, may not increase with future climate change unless there are associated reductions in cloud cover. Thus far, there is no evidence of long-term changes in cloud cover at BCI (Pau et al. 2013). Additionally, it is possible that increasing GPP at cooler temperatures may offset declines at high temperatures, and thus, the net outcome for GPP at this site is unclear. Afternoon declines in GPP occur in many flux tower sites, with peak VPD in the afternoon strongly controlling stomatal closure (Lasslop et al. 2010).

T_{can} inherently captures aspects of the canopy's response to VPD and radiation (and non-steady-state responses to the environment such as wind speed), resulting in better prediction of GPP at this site. However, the underlying mechanisms driving T_{can} may shift from morning to afternoon (i.e., evaporative cooling to sensible heat loss). T_{can} furthermore integrates a diversity of species in a biologically complex tropical forest comprised of different surfaces (bark and flowers) and species with different leaf traits. Thus, greater evaporative cooling, which kept maximum T_{can} lower in the mornings, is in part driven by the relative abundance of species that have the ability to increase latent heat loss by having high stomatal conductance or the ability to limit sensible heat gain by having large leaves with a large boundary layer resistance. Species can also lower leaf temperatures by, for example, decreasing net radiation absorbed through differences in leaf angle, pubescence, and leaf waxes. Deciduous species on the other hand represent an avoidance strategy by dropping leaves during the dry season when conditions at BCI are warmer, drier, and sunnier. Canopy temperature differences associated with different species composition should also help refine our understanding of the biophysical impacts of changing forest cover on local climate conditions (e.g., Bonan 2008, Luyssaert et al. 2014, Li et al. 2015).

Our study examines the effect of T_{can} on GPP—the rate of carbon fixed by the forest during photosynthesis—but large uncertainty remains regarding the effect of temperature on plant respiration and resulting NPP, that is, the net amount of carbon fixed and accumulated as plant biomass. Satellite-derived NPP has revealed decreasing trends across the tropical forest biome between ~2000 and 2010 (e.g., Zhao and Running 2010, Cleveland et al. 2015), while process models predict a long-term increase in NPP (Cleveland et al. 2015). Accurate projections of carbon cycling for the tropical forest biome will require direct field measurements from representative sites to capture landscape-level variability, over a sufficiently long time (Clark et al. 2017). To complement such large-scale analyses, continuous, high-resolution measurements of in situ canopy temperatures, such as described here, will be critical to understanding diverse canopy responses to rapid climate warming expected in coming years.

Acknowledgments

We thank Helene Mueller-Landau, Martijn Slot, and Geetha Iyer for their assistance with field work and instrumentation. This work was supported by the Department of Geography at Florida State University, the College of Forestry at Oregon State University, and the Macrosystems Biology Program of the National Science Foundation (Award No.: 1241953) to C.J.S.

Literature Cited

Aubrecht, D. M., B. R. Helliker, M. L. Goulden, D. A. Roberts, C. J. Still, and A. D. Richardson. 2016. Continuous, long-term, high-frequency thermal imaging of vegetation: uncertainties and recommended best practices. Agricultural and Forest Meteorology 228–229:315–326.

Battisti, D. S., and R. L. Naylor. 2009. Historical warnings of future food insecurity with unprecedented seasonal heat. Science 323:240–244.

Bonan, G. B. 2008. Forests and climate change: forcings, feedbacks, and the climate benefits of forests. Science 320:1444–1449.

Briscoe, N. J., K. A. Handasyde, S. R. Griffith, W. P. Porter, A. Krockenberger, and M. R. Kearney. 2014. Tree-hugging koalas demonstrate a novel thermoregulatory mechanism for arboreal mammals. Biology Letters 10:20140235.

Burnham, K. P., and D. R. Anderson. 2002. Model selection and multimodel inference: a practical information-theoretic approach. Second edition. Springer, New York, New York, USA.

Cheesman, A. W., and K. Winter. 2013. Elevated nighttime temperatures increase growth in seedlings of two tropical pioneer tree species. New Phytologist 197:1185–1192.

Clark, D. A., S. Asao, R. Fisher, S. Reed, P. B. Reich, M. G. Ryan, T. E. Wood, and X. Yang. 2017. Field data to benchmark the carbon-cycle models for tropical forests. Biogeosciences 14:4663–4690.

Clark, D. B., D. A. Clark, and S. F. Oberbauer. 2010. Annual wood production in a tropical rain forest in NE Costa Rica linked to climatic variation but not to increasing CO2. Global Change Biology 16:747–759.

Clark, D. A., D. B. Clark, and S. F. Oberbauer. 2013. Field-quantified responses of tropical rainforest aboveground productivity to increasing CO2 and climatic stress, 1997-2009. Journal of Geophysical Research: Biogeosciences 118:783–794.

Clark, D. A., S. C. Piper, C. D. Keeling, and D. B. Clark. 2003. Tropical rain forest tree growth and atmospheric carbon dynamics linked to interannual temperature variation during 1984–2000. Proceedings of the National Academy of Sciences of the United States of America 100:5852–5857.

Cleveland, C. C., P. Taylor, K. D. Chadwick, K. Dahlin, C. E. Doughty, Y. Malhi, W. K. Smith, B. W. Sullivan, W. R. Wieder, and A. R. Townsend. 2015. A comparison of plot-based satellite and Earth system model estimates of tropical forest net primary production. Global Biogeochemical Cycles 29:626–644.

Croat, T. B. 1978. Flora of Barro Colorado island. Stanford University Press, Stanford, California, USA.

Detto, M., D. Baldocchi, and G. G. Katul. 2010. Scaling properties of biologically active scalar concentration fluctuations in the atmospheric surface layer over a managed peatland. Boundary-Layer Meteorology 136:407–430.

Diffenbaugh, N. S., and M. Scherer. 2011. Observational and model evidence of global emergence of permanent, unprecedented heat in the 20th and 21st centuries. Climatic Change 107:615–624.

Doughty, C. E. 2011. An "In Situ "leaf and branch warming experiment in the Amazon. Biotropica 43:658–665.

Doughty, C. E., and M. L. Goulden. 2008. Are tropical forests near a high temperature threshold? Journal of Geophysical Research 113:1–12.

Faye, E., O. Dangles, and S. Pincebourde. 2016. Distance makes the difference in thermography for ecological studies. Journal of Thermal Biology 56:1–9.

Fisher, J. B., R. J. Whittaker, and Y. Malhi. 2011. ET come home: potential evapotranspiration in geographical ecology. Global Ecology and Biogeography 20:1–18.

Ghalambor, C. K., R. B. Huey, P. R. Martin, J. J. Tewksbury, and G. Wang. 2006. Are mountain passes higher in the tropics? Janzen's hypothesis revisited. Integrative and Comparative Biology 46:5–17.

Hagan, M. T., and M. Menhaj. 1994. Training feedforward networks with the Marquardt algorithm. IEEE Transactions on Neural Networks 5:989–993.

IPCC. 2014. Climate change 2014: synthesis report. Contribution of working groups I, II and III to the Fifth assessment report of the intergovernmental panel on climate change. *In* Core Writing Team, R. K. Pachauri and L. A. Meyer, editors. IPCC, Geneva, Switzerland, 151 pp.

Jacobson, M. Z. 2002. Fundamentals of atmospheric modeling. Cambridge University Press, New York, New York, USA.

Janzen, D. H. 1988. Why mountain passes are higher in the tropics. American Naturalist 101:233–249.

Jones, H. G. 1992. Plants and microclimate. Cambridge University Press, Cambridge, UK.

Kaspari, M., N. A. Clay, J. Lucas, S. P. Yanoviak, and A. Kay. 2015. Thermal adaptation generates a diversity of thermal limits in a rainforest ant community. Global Change Biology 21:1092–1102.

Kim, Y., C. J. Still, C. V. Hanson, H. Kwon, B. T. Greer, and B. E. Law. 2016. Canopy skin temperature variations in relation to climate, soil temperature, and carbon flux at a ponderosa pine forest in central Oregon. Agricultural and Forest Meteorology 226–227:161–173.

Lasslop, G., M. Reichstein, D. Papale, A. Richardson, A. Arneth, A. Barr, P. Stoy, and G. Wohlfahrt. 2010. Separation of net ecosystem exchange into assimilation and respiration using a light response curve approach: critical issues and global evaluation. Global Change Biology 16:187–208.

Leuzinger, S., and C. Körner. 2007. Tree species diversity affects canopy leaf temperatures in a mature temperate forest. Agricultural and Forest Meteorology 146:29–37.

Li, Y., M. Zhao, S. Motesharrei, Q. Mu, E. Kalnay, and S. Li. 2015. Local cooling and warming effects of

forests based on satellite observations. Nature Communications 6:6603.

Luyssaert, S. 2014. Land management and land-cover change have impacts of similar magnitude on surface temperature. Nature Climate Change 4:389–393.

Luyssaert, S., et al. 2014. Land management and land-cover change have impacts of similar magnitude on surface temperature. Nature Climate Change 4:389–393.

Mildrexler, D. J., M. Zhao, and S. W. Running. 2011. A global comparison between station air temperatures and MODIS land surface temperatures reveals the cooling role of forests. Journal of Geophysical Research: Biogeosciences 116:1–15.

Minkina, W., and S. Dudzik. 2006. Simulation analysis of uncertainty of infrared camera measurement and processing path. Journal of the International Measurement Confederation 39:758–763.

Mora, C., et al. 2013. The projected timing of climate departure from recent variability. Nature 502:183–187.

Pan, Y., et al. 2011. A large and persistent carbon sink in the world's forests. Science 333:988–993.

Papale, D., and R. Valentini. 2003. A new assessment of European forests carbon exchanges by eddy fluxes and artificial neural network spatialization. Global Change Biology 9:525–535.

Pau, S., D. K. Okamoto, S. J. Wright, and O. Calderon. 2018. Long-term increases in tropical flower production across growth forms in response to Anthropogenic climate change. Global Change Biology 24:2105–2116.

Pau, S., E. M. Wolkovich, B. I. Cook, C. J. Nytch, J. Regetz, J. K. Zimmerman, and S. Joseph Wright. 2013. Clouds and temperature drive dynamic changes in tropical flower production. Nature Climate Change 3:838–842.

Rey-Sánchez, A., M. Slot, J. Posada, and K. Kitajima. 2016. Spatial and seasonal variation in leaf temperature within the canopy of a tropical forest. Climate Research 71:75–89.

Scherrer, D., and C. Körner. 2011. Topographically controlled thermal-habitat differentiation buffers alpine plant diversity against climate warming. Journal of Biogeography 38:406–416.

Slot, M., C. Rey-Sánchez, S. Gerber, J. W. Lichstein, K. Winter, and K. Kitajima. 2014. Thermal acclimation of leaf respiration of tropical trees and lianas: response to experimental canopy warming, and consequences for tropical forest carbon balance. Global Change Biology 20:2915–2926.

Slot, M., and K. Winter. 2017*a*. In situ temperature response of photosynthesis of 42 tree and liana species in the canopy of two Panamanian lowland tropical forests with contrasting rainfall regimes. New Phytologist 214:1103–1117.

Slot, M., and K. Winter. 2017*b*. In situ temperature relationships of biochemical and stomatal controls of photosynthesis in four lowland tropical tree species. Plant, Cell & Environment 2017:1–14.

Still, C. J., S. Pau, and E. J. Edwards. 2014. Land surface skin temperature captures thermal environments of C3 and C4 grasses. Global Ecology and Biogeography 23:286–296.

Tewksbury, J. J., R. B. Huey, and C. A. Deutsch. 2008. Putting the heat on tropical animals. Science 320:1296–1297.

Toomey, M., D. A. Roberts, C. Still, M. L. Goulden, and J. P. McFadden. 2011. Remotely sensed heat anomalies linked with Amazonian forest biomass declines. Geophysical Research Letters 38:1–5.

Turner, W. 2014. Sensing biodiversity. Science 346:301–302.

Vancutsem, C., P. Ceccato, T. Dinku, and S. J. Connor. 2010. Evaluation of MODIS land surface temperature data to estimate air temperature in different ecosystems over Africa. Remote Sensing of Environment 114:449–465.

Wright, S. J., H. C. Muller-Landau, and J. A. N. Schipper. 2009. The future of tropical species on a warmer planet. Conservation Biology 23:1418–1426.

Woods, C. L., C. L. Cardelús, and S. J. Dewalt. 2015. Microhabitat associations of vascular epiphytes in a wet tropical forest canopy. Journal of Ecology 103:421–430.

Zhao, M., and S. W. Running. 2010. Drought-induced reduction in global terrestrial net primary production from 2000 through 2009. Science 329:940–943.

Supporting Information

Additional Supporting Information may be found online at: http://onlinelibrary.wiley.com/doi/10.1002/ecs2.2311/full